Research Report
2011-24

Experimental Evaluation of a Doubly-Fed Linear Generator for Ocean Wave Energy Applications

J. Vining, T.A. Lipo, G. Venkataramanan

Dept. of Elect. & Comp. Engr.
University of Wisconsin-Madison
1415 Engineering Drive
Madison, WI 53706

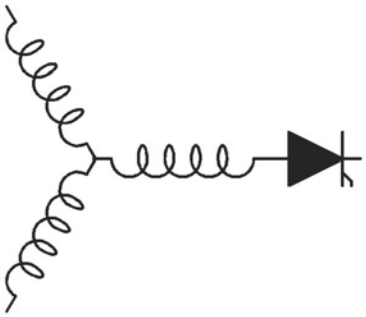

Wisconsin
Electric
Machines &
Power
Electronics
Consortium

University of Wisconsin-Madison
College of Engineering
Wisconsin Power Electronics Research Center
2559D Engineering Hall
1415 Engineering Drive
Madison WI 53706-1691

Experimental Evaluation of a Doubly-Fed Linear Generator for Ocean Wave Energy Applications

J. Vining, T.A. Lipo, G. Venkataramanan
Department of Electrical and Computer Engineering
University of Wisconsin - Madison
Madison, WI, USA
vining@wisc.edu, lipo@engr.wisc.edu, giri@engr.wisc.edu

***Abstract*—A versatile doubly-fed linear generator was recently presented for application in the point absorber ocean wave energy converter (WEC). Whereas this machine may be operated as a singly- or doubly-fed induction machine or via a self-synchronous approach, operation as a synchronous machine is found to be an attractive method for experimental testing. Using this mode of operation, the generator may be run with a DC field in either the translator or stator, thus producing power from the stator or translator respectively. Given the unique hybrid-flux architecture of this linear generator, synchronous testing in this manner provides a way to quantify the difference in electrical and reactive force production between the translator and stator topologies under WEC operating conditions, i.e. low speed with high force. This paper presents the testing procedure and setup along with detailed prototype results.**

Keywords - ocean wave energy conversion; linear generator; doubly-fed linear machine control; alternative energy conversion

I. INTRODUCTION

In wave energy converter (WEC) applications, direct drive power take-off is less mechanically complex than hydraulic- or pneumatic-based systems and thus has the opportunity for superior performance and increased efficiency [1-4]. A prototype of such a direct drive system has been constructed and tested. The prototype machine is based on the novel hybrid-flux linear generator design developed in [5], while the testing procedure is meant to build towards the self-synchronous control method specially designed for this machine architecture in [6]. A basic representation of one pole-pair of the machine topology is illustrated in Fig. 1, and a picture of the test bench construction is shown in Fig. 2.

The prototype machine is tested in the synchronous mode to quantify electrical and reactive force production differences between the stator and translator flux topologies. Section II describes the equipment and test bench setup while Section III provides an explanation of the test procedure. This is followed by experimental prototype results in Section IV. The experimental results highlight stator/translator topology distinctions with respect to open circuit voltage (Section IV.A), short circuit current (Section IV.B), synchronous inductance (Section IV.B), output power (Sections IV.C), force production (Sections IV.C), and efficiency (Section IV.D). A comparison with theoretical performance predictions in provided in Section IV.C.

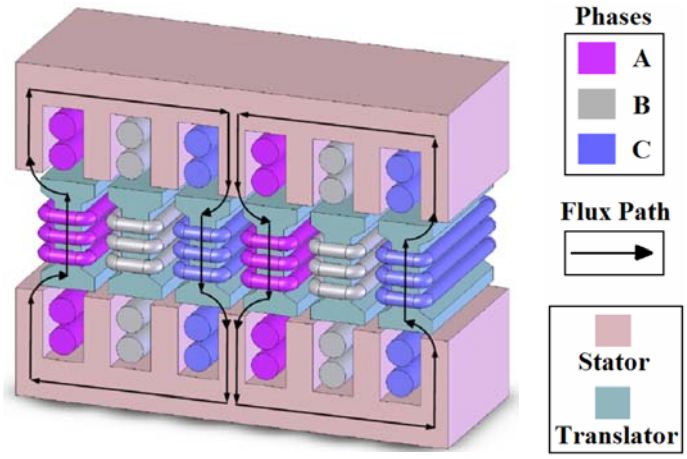

Figure 1. Flux Path for One Pole Pair (q_s=1, q_r=1) of the Hybrid Transverse / Longitudinal Flux Linear Wound-Field Generator from [1]

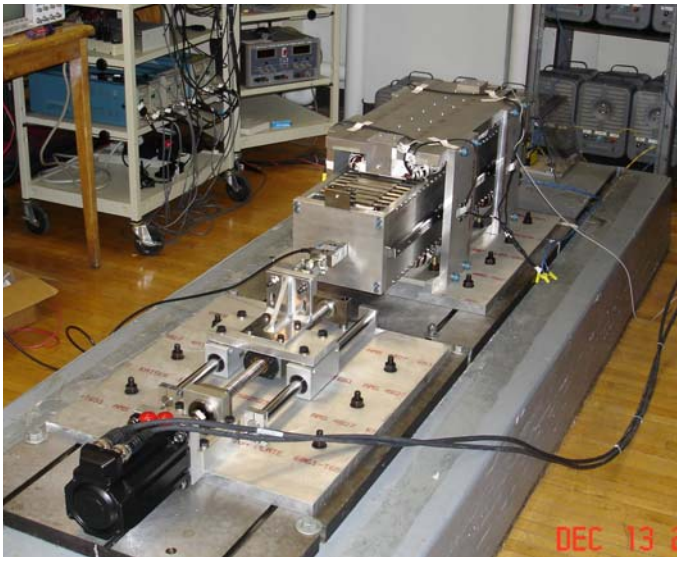

Figure 2. Test Bench for Experimental Analysis of the Prototype

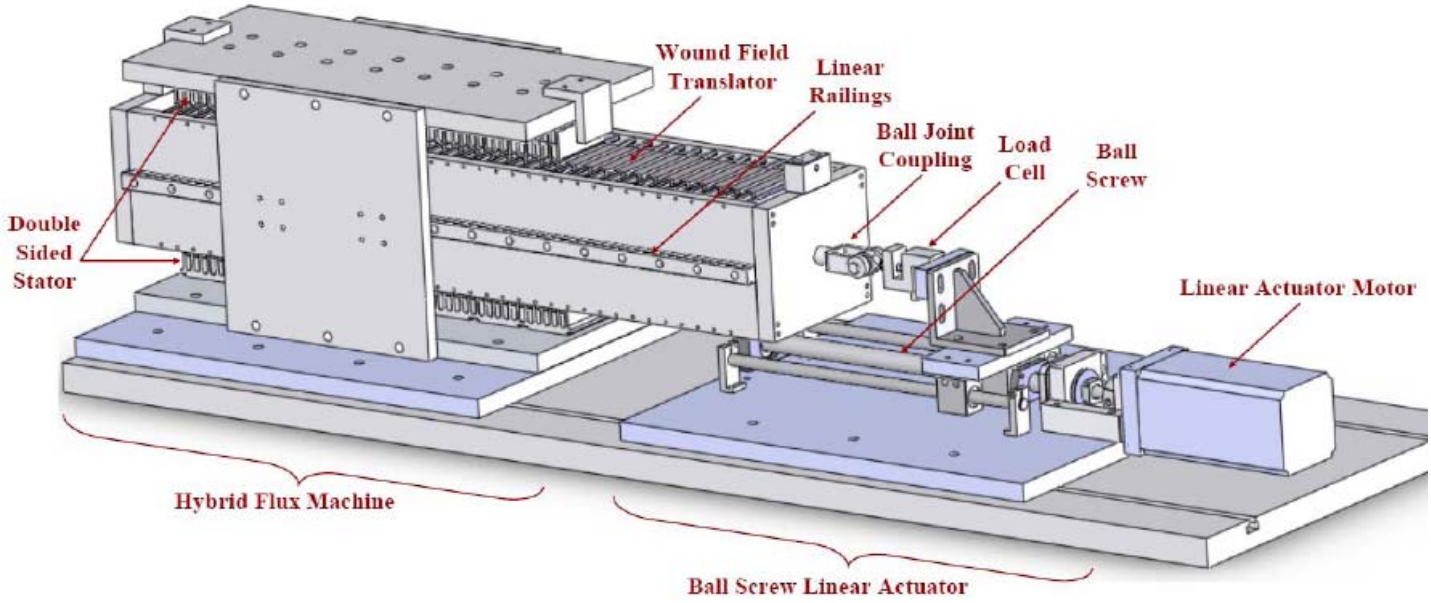

Figure 3. SolidWorks Sketch of the Test Bench Setup with Annotations

II. Equipment and Test Bench Setup

An annotated sketch of the test bench setup is pictured in Fig. 3. This sketch pinpoints major components in addition to showing how the generator is connected to the dynamometer (the ball screw linear actuator).

Ratings of the test machine and the dynamometer are listed in Table I and Table II respectively.

A few important points related to the test setup include:

- The rated force and speed of the dynamometer is less than that of the test machine which limits the testing range.
- *DE-RATING:* Although the design in [5] dictates a copper fill factor of 50% in the stator, this was not achieved in the test machine. Thus, the rated peak current is 14 A.
- Unlike conventional rotary machines, a direct electrical connection may be made with the translator via a flexible retractile cable rather than through slip rings. As such, the translator currents are sensed directly.
- Voltage, current, force, and position data are acquired via a LabVIEW module.
- Position feedback is provided by the servo motor drive by means of an analog output signal.
- The load cell is placed in line between the translator and dynamometer and thus reads both reactive and friction forces.
- The stroke length comprises roughly 3.8 poles, nearly two pole pairs.

TABLE I. Characteristics of Test Machine from [5]

Parameter	Symbol	Value	Units
Rated Line-Line Voltage	$V_{RMS,LL}$	230	(V_{RMS})
Rated Peak Current	I_{pk}	14	(A)
Number of Poles	P	8	(-)
Stator Resistance	r_s	6.3	(Ω)
Translator Resistance	r_r	6.1	(Ω)
Rated Speed	v_{stroke}	1.4	(m/s)
Stator Pole Pitch	$\tau_{s,pole}$	0.078	(m)
Active (Airgap) Area	A_{airgap}	0.1248	(m^2)
Stroke Length	l_{stroke}	0.3	(m)

† Original current rating is 20 A; due to limited copper fill factor of prototype

TABLE II. Characteristics of Linear Actuator Dynamometer

Parameter	Value	Units
Rated Speed †	1.25	(m/s)
Rated Force ††	3.37	(kN)
Stroke Length	0.3	(m)

† Limited by motor speed and ball screw lead
†† Limited by ball screw bearings

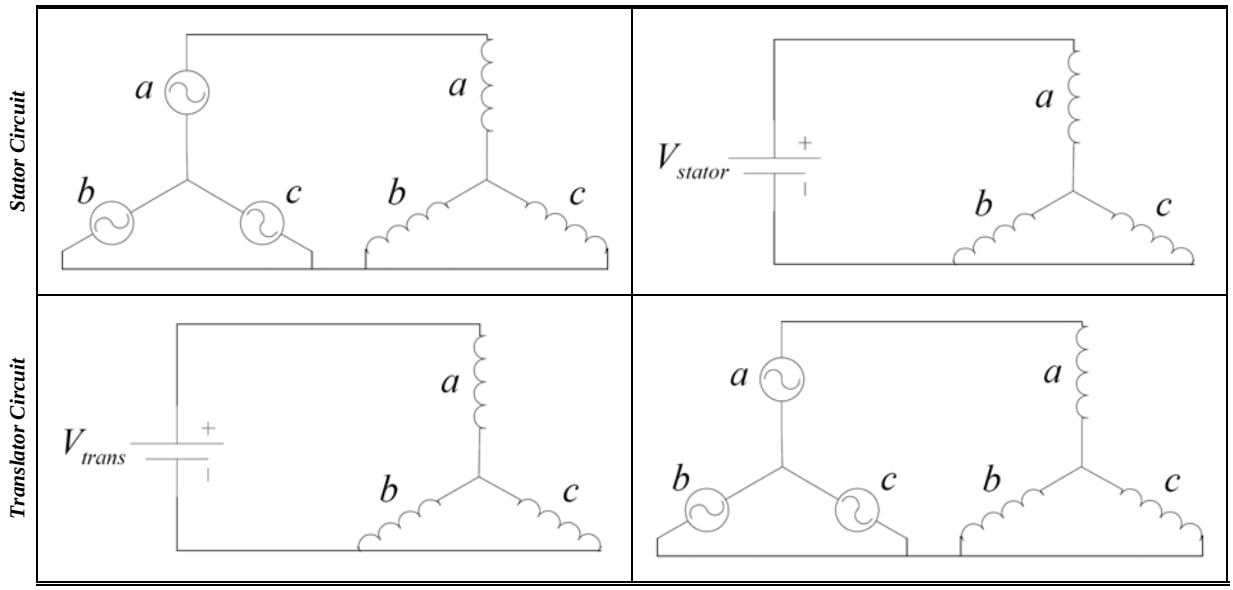

(a) DC on the translator, AC electrical output from the stator

(b) DC on the stator, AC electrical output from the translator

Figure 4. DC Excitation Circuits for the Synchronous Generator Test

III. Test Procedure

The generator is run in two synchronous operating modes: 1) DC on the translator and 2) DC on the stator. The excitation circuits used to produce these DC fields are presented in Fig. 4. This serves the purpose of quantifying electrical and reactive force production differences between the translator and stator topologies.

Each test is conducted at differing levels of DC field flux to examine the effect of flux level on power and reactive force production. It is expected that force production will be proportional to the field flux as indicated in (1) given that the machine is not in saturation. By extension, power should also be proportional to the field flux since power is equal to the product of mechanical velocity and force (see equations (2) and (3)). For these tests, the generator is loaded electrically with a resistor bank in order to gauge electrical output power.

For each field flux level, the translator will be driven at several discrete velocities as well as sinusoidal velocity trajectories. A position feedback signal is taken from the dynamometer drive for comparison. Operation at each discrete velocity allows for measurement of steady-state force and power at a given field flux. It is expected that the generated power is proportional to the velocity, provided that the machine is not in saturation. The sinusoidal velocity trajectories are chosen to mimic a direct-drive wave energy converter application with limited stroke length. The dynamic response of the sinusoidal trajectory is compared against the steady-state values.

$$F \propto \Phi_{field}. \tag{1}$$

$$P = v_{trans} F. \tag{2}$$

$$P \propto \Phi_{field}. \tag{3}$$

IV. Experimental Generator Performance Characterization

The experimental results that follow include open circuit voltage, short circuit current, output power, force production, and efficiency with the DC field in either the stator or translator. The power and force production tests are performed at steady state single velocities in addition to dynamic sinusoidal velocities. All of this is compared to theoretical steady state performance using the machine model in Fig. 5.

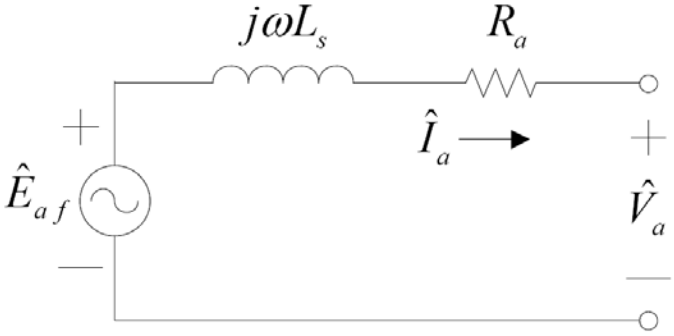

Figure 5. Per Phase Steady State Synchronous Machine Equivalent Circuit

A. Open Circuit Voltage

1) Steady State Open Circuit Voltage

In this test, the machine is run at a discrete speed with a discrete DC field. Given that the output terminals are open circuited, the terminal voltage reads the back emf, E_{af}, produced by the DC field at that particular operating point.

Figs. 6 and 7 chart the open circuit voltage of the test machine with the DC field applied to stator and translator respectively.

A few points are worth mentioning with regards to the open circuit test:

- Under these conditions, the machine operates in the unsaturated region since the voltage does not decay with increased speed or field strength.
- Applying the DC field to the translator tends to produce a higher back emf on average.
- The open circuit voltage is linearly related to both the speed and field flux as predicted in Section III.

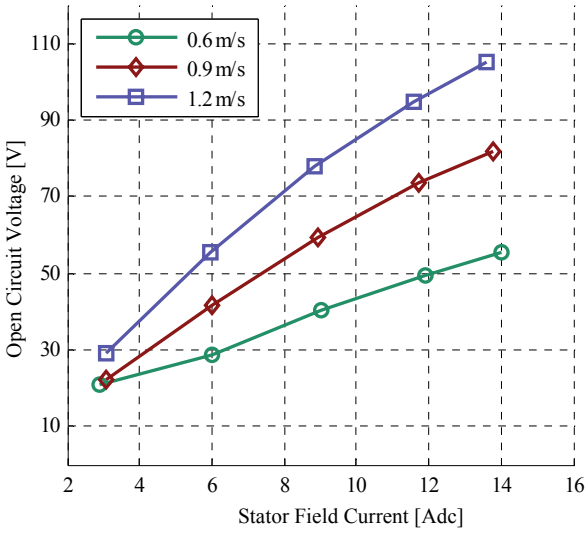

Figure 6. Steady State Open Circuit Voltage with Stator Field

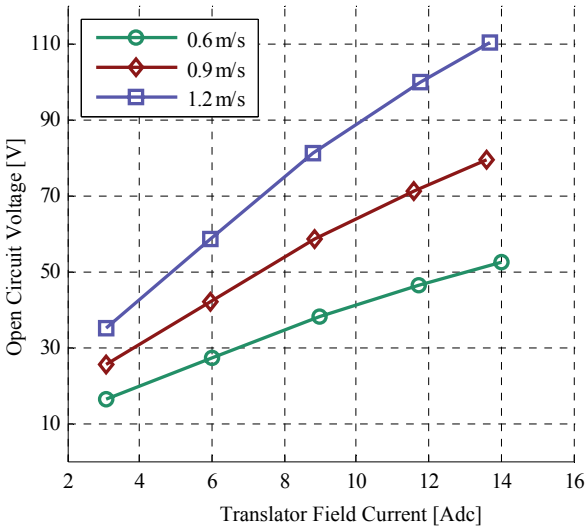

Figure 7. Steady State Open Circuit Voltage with Translator Field

2) Open Circuit Voltage under Sinusoidal Motion

While the open circuit test charts E_{af} at several discrete speeds, it is of interest to show how the open circuit voltage varies if a sinusoidal velocity is imposed on the machine. Figs. 8 and 9 illustrate this operating condition.

Two conclusions should be drawn from Figs. 8 and 9:

- The voltage varies linearly with the applied speed.
- The voltage alternates between positive and negative sequence depending on the velocity.

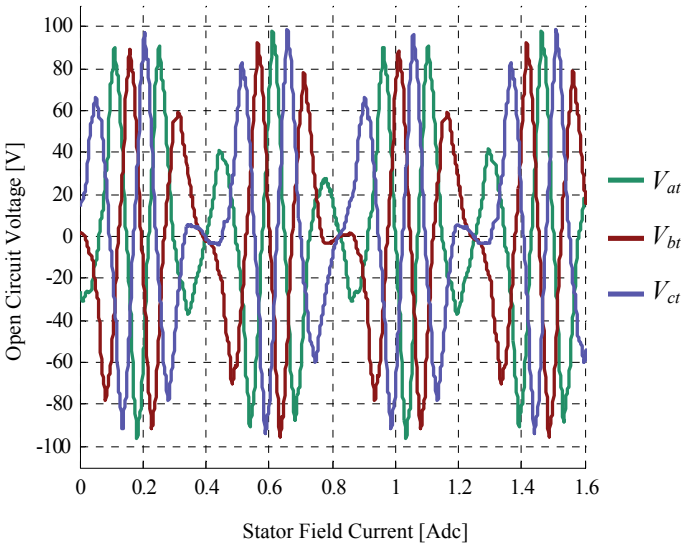

Figure 8. Open Circuit Voltage with Stator Field given a Sinusoidal Velocity with Peak Speed of 1.2 m/s

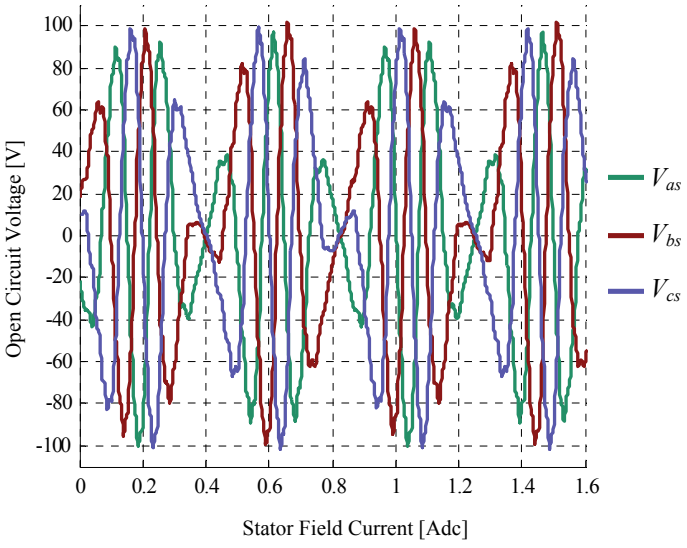

Figure 9. Open Circuit Voltage with Stator Field given a Sinusoidal Velocity with Peak Speed of 1.2 m/s

B. Steady State Short Circuit Current

As with the steady state open circuit test, the machine is run at a discrete speed with a discrete DC field; however, the output terminals are short circuited. Figs. 10 and 11 chart the short circuit current of the test machine with the DC field applied to stator and translator respectively. Similar to the open circuit test, the short circuit current varies linearly with the speed and field intensity. Also, applying the DC field to the translator tends to produce a higher short circuit current on average.

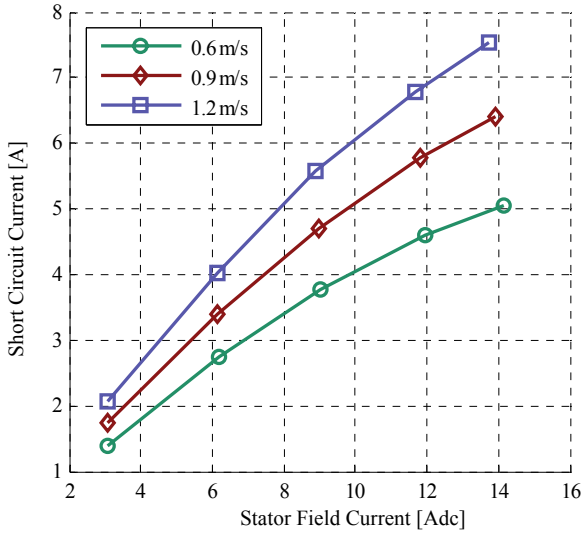

Figure 10. Steady State Short Circuit Current with Stator Field

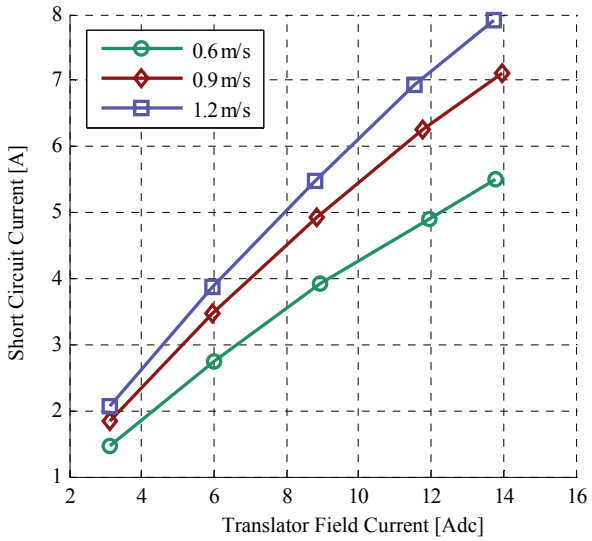

Figure 11. Steady State Short Circuit Current with Translator Field

1) Calculating Synchronous Inductance from Short Circuit Data

Given that V_a = 0 during short circuit operation, it is apparent that the synchronous inductance may be found using the steady state machine equation (4). Typical calculations of synchronous inductance, see equation (5), neglect the armature resistance, R_a [7], yet resistance plays a larger role in this machine due to the greater number of winding turns. By calculating the synchronous inductance with relatively low short circuit current conditions, it is possible to use (5) since the effect of the resistive component is minimized. These results are presented in Table III.

$$\hat{V}_a = -R_a\hat{I}_a - j\omega L_s\hat{I}_a + \hat{E}_{af}. \quad (4)$$

$$\omega L_s = \frac{E_{af}}{I_{\substack{short\\ckt}}}. \quad (5)$$

TABLE III. SYNCHRONOUS INDUCTANCE

Parameter	Value	Units
Synchronous Inductance with Stator Field	0.45	(H)
Synchronous Inductance with Translator Field	0.42	(H)

C. *Steady State Output with Electrical Loading*

In this section the machine performance is measured both theoretically and experimentally with respect to electrical loading.

1) Power Output Sensitivity to Electrical Loading

Using the synchronous inductance values from Table III and the steady state machine equation (4), operating conditions for various loadings can be derived. Fig. 12 illustrates the steady state output power for load resistances up to100Ω. For both stator and translator fields R_{load} of approximately 20Ω produces maximum power. As such, experimental tests use 20Ω loading.

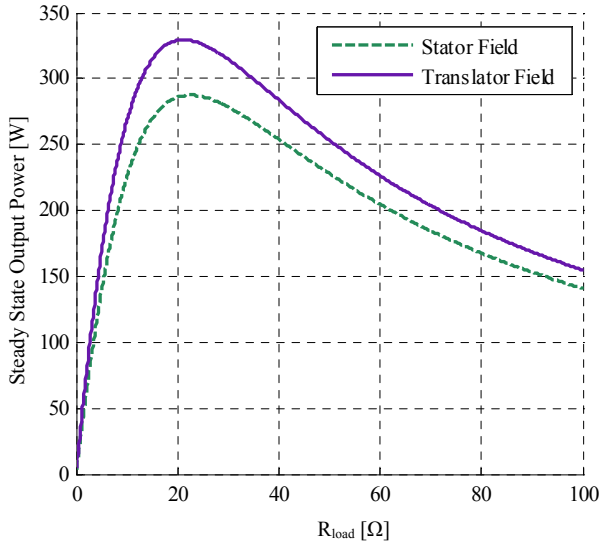

Figure 12. Steady State Output Power with varying R_{load} when I_{field} = 14 A and v_{stroke} = 1.2 m/s

2) Power and Force Production with Electrical Loading

As shown in Fig. 12, a load resistance of approximately 20Ω produces maximum steady state output power. This electrical loading is used in the experimental data shown in Figs. 13, 14, 15, and 16.

Figs. 13 and 14 show both the experimental (solid line) and theoretical (hashed line) electrical output power at this loading with stator and translator fields respectively. Figs. 15 and 16 illustrate experimental reactive force production. It can be concluded from these figures that:

- The steady state model accurately reflects the experimental data.
- Applying the DC field to the translator tends to produce larger output power yet lower reactive force, especially at higher speeds.

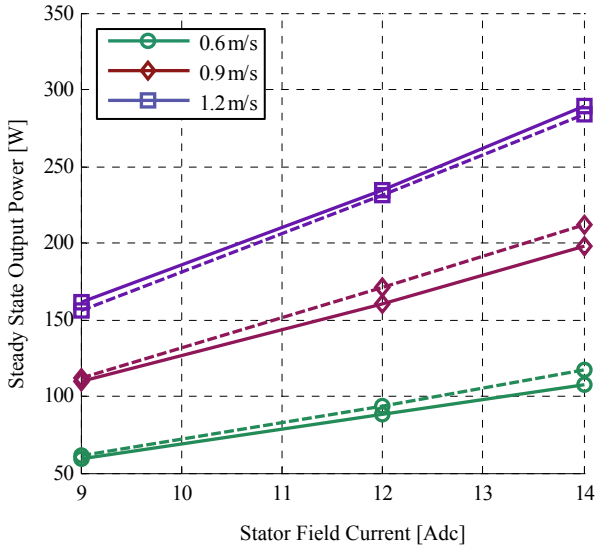

Figure 13. Steady State Output Power at R_{load} = 20Ω with Stator Field (*Solid Line is Experimental, Hash Line is Theoretical*)

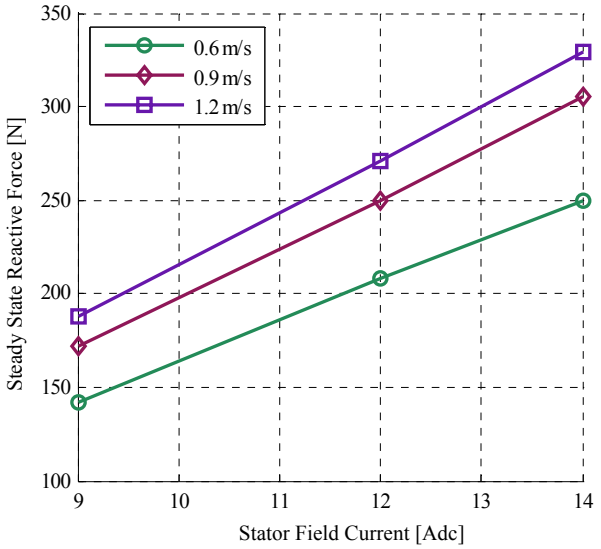

Figure 15. Experimental Steady State Reactive Force at R_{load} = 20Ω with Stator Field

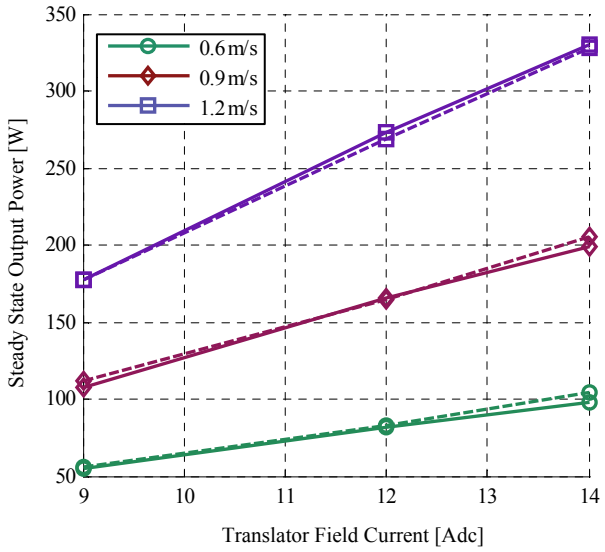

Figure 14. Steady State Output Power at R_{load} = 20Ω with Translator Field (*Solid Line is Experimental, Hash Line is Theoretical*)

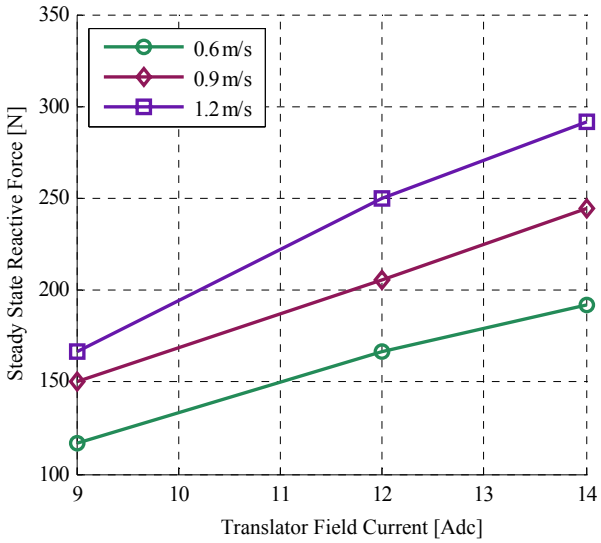

Figure 16. Experimental Steady State Reactive Force at R_{load} = 20Ω with Translator Field

D. Steady State Efficiency

The machine efficiency can be calculated via equation (6) using data from the previous section. The input power only accounts for the external force required to move the translator and not the field power. Efficiency data is presented in Figs. 17 and 18.

$$\eta_{eff} = \frac{P_{out}}{P_{in}} = \frac{\sum_{x=a,b,c} I_x V_x}{v_{stroke} F}. \qquad (6)$$

The following trends appear in Figs. 17 and 18:

- Efficiency increases with increasing velocity and field intensity.
- As would be expected due to its higher power production and lower reactive force, a translator DC field yields higher efficiency than a stator DC field.

The efficiency would be expected to level off at greater output power levels [8].

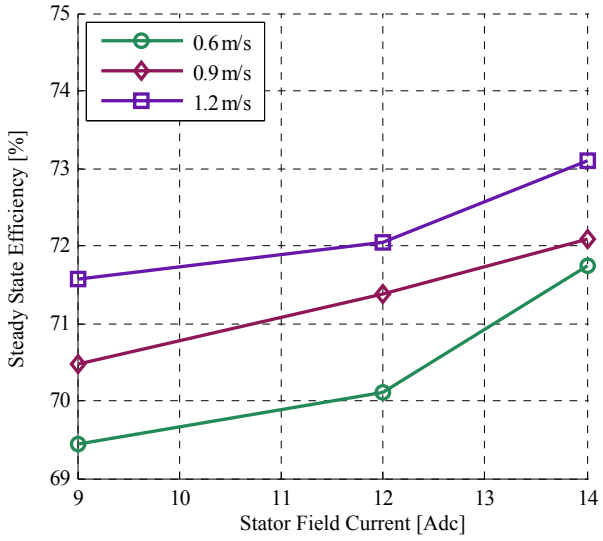

Figure 17. Steady State Operating Efficiency with R_{load} = 20Ω and Stator Field

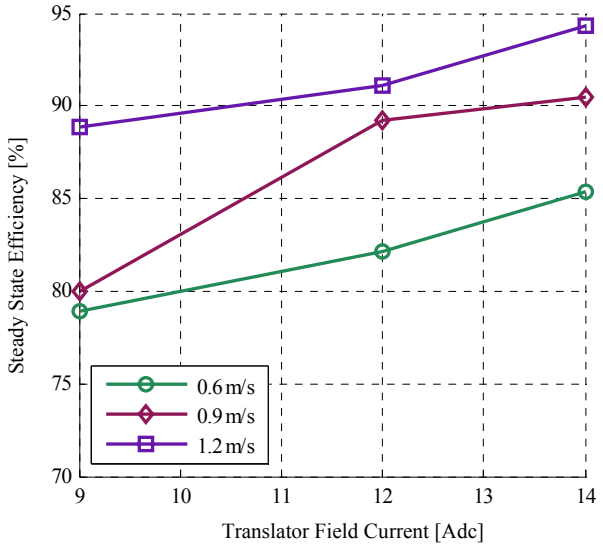

Figure 18. Steady State Operating Efficiency with R_{load} = 20Ω and Translator Field

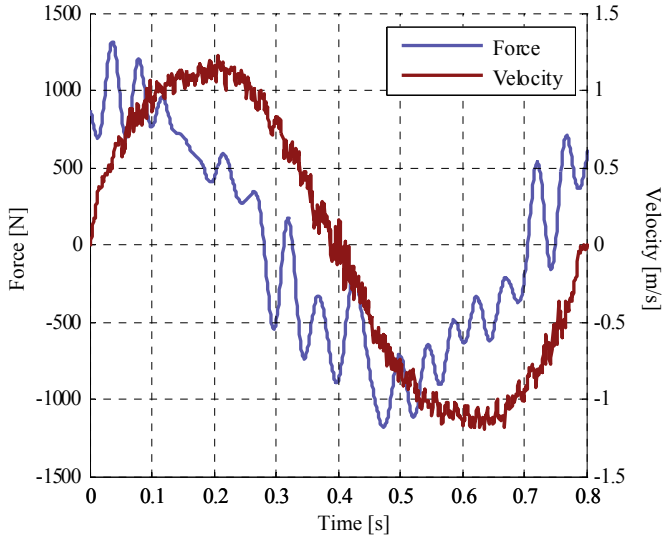

Figure 19. Force and Velocity with Stator Field for R_{load} = 20Ω

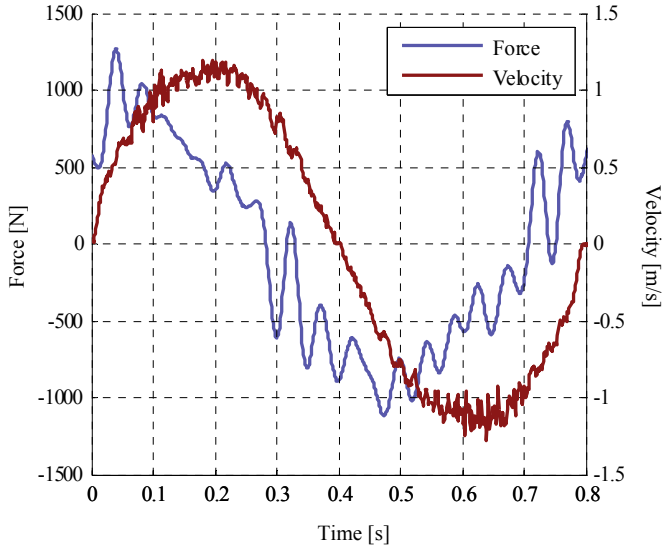

Figure 20. Force and Velocity with Translator Field for R_{load} = 20Ω

E. Generator Performance under Sinusoidal Motion

Whereas previous sections have documented the performance of this test machine under steady state operating conditions, this section documents performance under sinusoidal motion. Although most sea states behave according to statistical models such as the Jonswap or Bretschneider spectrums, the sinusoidal velocity imposed here is meant to mimic wave motion.

In this analysis, the power and force production are of most interest. As such, Figs. 19 and 20 plot the reactive force and velocity trajectory while Figs. 21 and 22 plot the output power.

A couple of statements can be made about operating under sinusoidal motion:

- While the force is proportional to the velocity, they are not in phase. An active control scheme that mitigates the inductive and resistive effects within the machine could improve power output by bringing the force in phase with the velocity.
- As with steady state operation, the power output with a translator field exceeds that of the stator field.
- The power output fluctuates sinusoidally with the velocity.
- The polarity of the velocity dictates whether the output power is positive or negative sequence.

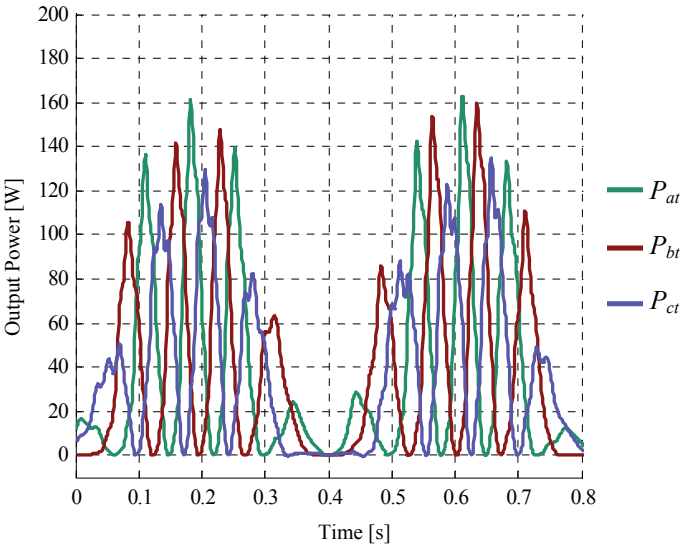

Figure 21. Output Power with Stator Field given the Sinusoidal Velocity in Fig. 19 with $R_{load} = 20\Omega$

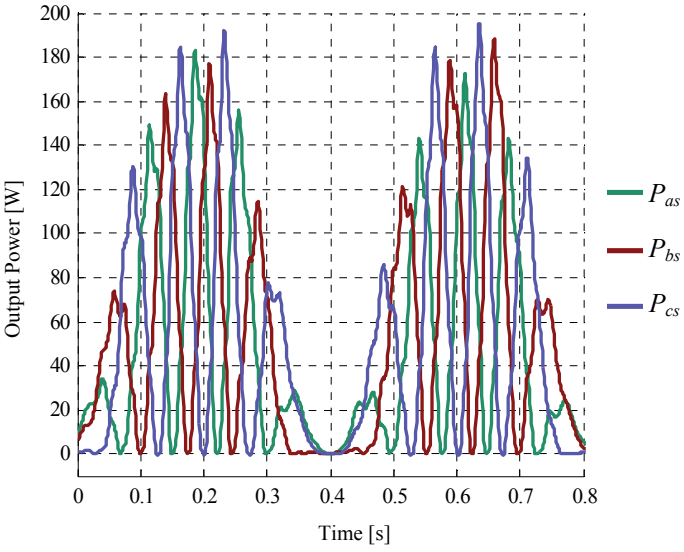

Figure 22. Output Power with Translator Field given the Sinusoidal Velocity in Fig. 20 with $R_{load} = 20\Omega$

V. CONCLUSIONS

This paper has documented a synchronous testing scheme for the doubly-fed linear machine introduced in [1]. Since the testing scheme involves applying a DC field alternately to the translator and then to the stator, characteristics unique to each are quantified in terms of power capture, reactive force production, and dynamic response. Based on experimental results, it can be said that a machine of this type is best configured with a translator DC field and a stator armature. This configuration yields higher efficiency and power capture for a given velocity and field intensity.

Future work in the area of control could increase power capture under dynamic loading as discussed in Section IV.E

ACKNOWLEDGMENTS

The authors would like to thank the support provided by the members of the Wisconsin Electric Machines and Power Electronics Consortium at the University of Wisconsin Madison. The expertise and guidance provided by members of the WEMPEC research group is greatly appreciated.

A special thanks goes to the Electrical Engineering Dept. at the University of Wisconsin - Madison for funding this project in part.

REFERENCES

[1] J.K.H. Shek, D.E. Macpherson, M.A. Mueller, "Experimental Verification of Linear Generator Control for Direct Drive Wave Energy Conversion," *IET Renewable Power Generation*, 2010, vol. 4, no. 5, pp. 395–403.

[2] M.A. Mueller, H. Polinder, N. Baker, "Current and Novel Electrical Generator Technology for Wave Energy Converters," *IEEE Electric Machines and Drives Conference*, 2007.

[3] A. Muetze and J.G.Vining, "Ocean Wave Energy Conversion – A Survey," *IEEE Industry Applications Society Conference*, 2007.

[4] R. Vermaak, M.J. Kamper, "Design of a Novel Air-Cored Permanent Magnet Linear Generator for Wave Energy Conversion," *IEEE International Conference on Electric Machines*, 2010.

[5] J.G.Vining, T.A. Lipo, and G.Venkataramanan, "Design and Optimization of a Novel Hybrid Transverse / Longitudinal Flux, Wound-Field Linear Machine for Ocean Wave Energy Conversion," *2009 IEEE Energy Conversion Congress and Exposition*, 20-24 September 2009.

[6] J.G.Vining, T.A. Lipo, and G.Venkataramanan, "Self-Synchronous Control of Doubly-Fed Linear Generators for Ocean Wave Energy Applications," *2010 IEEE Energy Conversion Congress and Exposition*, 12-16 September 2010.

[7] A.E. Fitzgerald, C. Kingsley, S.D. Umans, *Electric Machinery*, 6th ed. New York: McGraw-Hill, 2003.

[8] C.S. Hoong and S. Taib, "Development of Three Phase Synchronous Generator for Ocean Wave Application," *National Power and Energy Conference*, 2003..